Journal of Structural Geology, Vol. 7, No. 6, pp. 667 to 682, 1985
Printed in Great Britain

0191-8141/85 $03.00 + 0.00

Mesoscopic structural fabric of early Paleozoic rocks in the northern Sierra Nevada, California and implications for Late Jurassic plate kinematics

ROBERT J. VARGA

Union Oil Research Center, Box 76, Brea, CA 92621, U.S.A.

(*Received* 5 *July* 1984; *accepted in revised form* 13 *February* 1985)

Abstract—Analysis of the mesoscopic structure of the early Paleozoic Shoo Fly complex, northern Sierra Nevada, California, reveals three phases of deformation and folding. The first phase of folding is pre-Late Devonian and the second two are constrained by regional relations as due to the Late Jurassic Nevadan orogeny. Main phase Nevadan deformation produced penetrative slaty cleavage which is steep, NNW-trending and parallel to tectonostratigraphic terranes of the region. Cleavage is axial-planar to ubiquitous isoclinal similar folds. Fold axes define a NNW-trending girdle with a distinct, near-vertical maximum. Main phase Nevadan folds have nearly ideal class 2 orthogonal thickness geometry although some class 1C forms exist in more competent units. The overall geometry of main phase folds suggests formation by progressive deformation in a flattening regime with cleavage as the flattening plane and a steep extension axis defined by the fold axis maximum. A steep extension axis direction for main phase Nevadan deformation is supported by analysis of interference relations where folds of this generation deform pre-Late Devonian folds. Late Nevadan folds range from kink flexures to ideal class 2 similar folds with incipient axial-planar cleavage. The kinematic significance of late Nevadan folds cannot be evaluated because of their varying style and orientation throughout the northern Sierra Nevada.

Penetrative ductile deformation and near-vertical extension during the Nevadan orogeny was synchronous with accretion of oceanic and/or island arc rocks against the western margin of the northern Sierra Nevada. The kinematic framework of deformation defined for Nevadan deformation is consistent with essentially orthogonal convergence of these exotic terranes with the Sierran margin and argues against a transform/transpressive regime.

INTRODUCTION

THE COMPLEX petrologic assemblages and structural geology of the Sierra Nevada range in California have inspired quite diverse tectonic models for this part of the North American Cordillera. However, on one point most authors agree; an intense period of orogenesis occurred during the mid-Mesozoic which produced penetrative structures and is responsible for the dominant NW-trending structural grain of the region (Fig. 1). This mid-Mesozoic deformation has become widely known as the 'Nevadan orogeny' (Taliaferro 1942), although the number and relative timing of parallel deformations usually ascribed to this event are controversial (Saleeby 1977, 1978, Tobisch & Fiske 1982).

Though the Nevadan orogeny is generally believed to be the direct result of accretion of ocean floor and/or island arc assemblages against the western margin of the North American craton, the nature of the accretionary process remains problematic. Two-dimensional models which depict perpendicular collision of oceanic terranes with the continental margin were first offered by Moores (1970) and have been subsequently elaborated on by a number of workers (e.g. Schweickert & Cowan 1975, Schweickert 1981, Moores & Day 1984). At the other end of the spectrum is a complex three-dimensional model suggested by Saleeby (1977, 1978, 1981). In his model, accretion is essentially non-collisional and attendant deformation of the continental margin is accomplished in a transpressive regime.

The gross geometry of relative motion (purely compressional, purely transform, or oblique 'transpression') between a continental margin and accreted terranes should have some expression in the type and geometry of structures produced during the accretionary process. The purpose of this paper is to describe the mesoscopic structural fabric imprinted upon early Paleozoic rocks of the northern Sierra Nevada during the Nevadan orogeny and to evaluate these structures as kinematic indicators of relative plate motions. Although the results of this analysis do not delineate second order complexities of motion between various fragments at the accreting margin, it is believed that the fabric described here will help discriminate between dominantly compressional and dominantly transform regimes.

GEOLOGIC SETTING OF THE NORTHERN SIERRA NEVADA

In the context of this paper, the northern Sierra Nevada range is that part of the range which lies north of about 39°N latitude. The geology of this part of the Sierra is divided into four distinct tectonostratigraphic terranes (Fig. 1). The mid-Paleozoic Feather River Peridotite belt (Ehrenberg 1975, Standlee 1978a) separates an Eastern belt of rocks, which are considered 'autochthonous' to the Mesozoic continental margin, from terranes to the west, which were accreted during phases of the Nevadan orogeny. Thus, the Feather River Peridotite belt demarks a fundamental break in this part of the Cordilleran margin which some workers have ascribed to early Mesozoic transform truncation or rifting (Schweickert 1976, Davis *et al.* 1978).

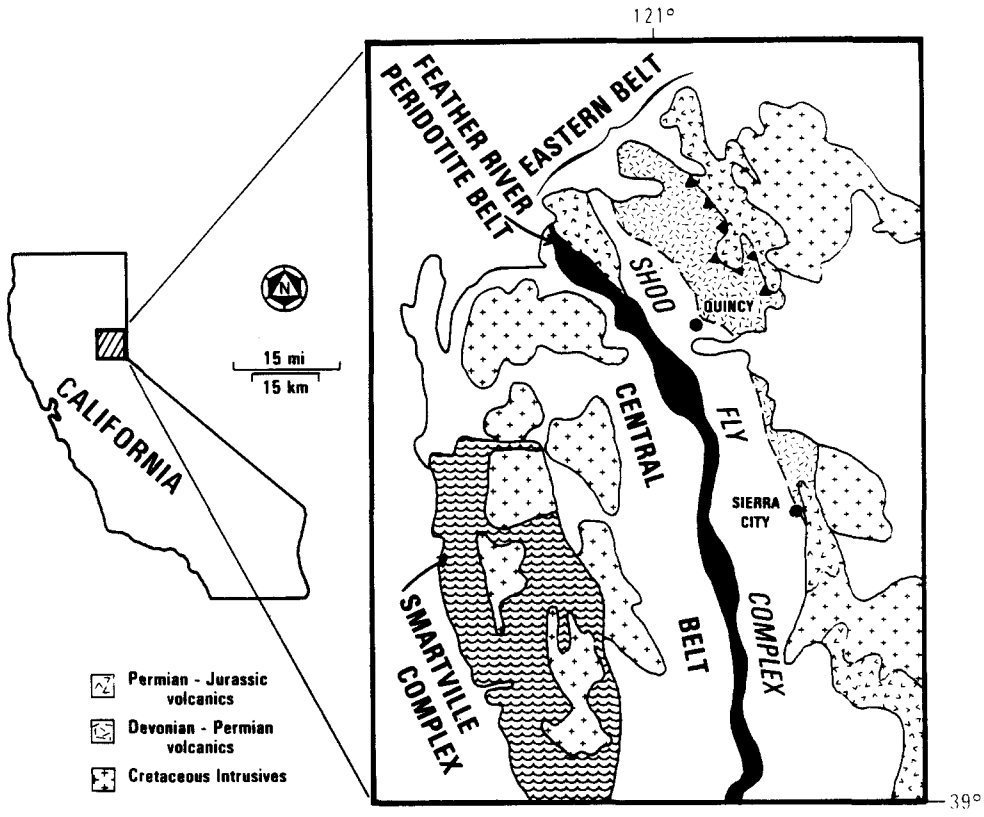

Fig. 1. Tectonostratigraphic terranes of the northern Sierra Nevada. Boundaries of units after Moores & Day (1984).

Rocks to the west of the Feather River Peridotite belt include the Smartville complex (Menzies *et al.* 1980) and a composite terrane known as the Central belt (e.g. Clark 1964, 1976, Hietanen 1981), both of which represent vestiges of Jurassic-age island arc and/or marginal basin oceanic crust (Moores & Day 1984, Tuminas 1983). To the east of the Feather River Peridotite belt is an Eastern belt, composed of lower Paleozoic siliciclastic sedimentary rocks of the Shoo Fly complex (Bond & Devay 1980, Varga & Moores 1981, Girty & Wardlaw 1984) which are unconformably overlain by mid-Paleozoic to Upper Jurassic volcanic arc assemblages (McMath 1966, Durrell & D'Allura 1977). All of these rocks were deformed and metamorphosed in Late Jurassic time (Hannah & Verosub 1980) and subsequently cut by Early Cretaceous plutons (Evernden & Kistler 1970). Contemporaneous metamorphism and deformation of both Eastern belt rocks and oceanic assemblages west of the Feather River Peridotite belt (Schweickert *et al.* 1984) strongly suggest a genetic link between Nevadan structures and accretion at the continental margin.

Early Paleozoic Shoo Fly Complex

The Shoo Fly complex north of the North Fork Yuba River (Fig. 2) is composed predominantly of phyllite and quartzose sandstone with minor amounts of chert, limestone, and silicic water-lain tuff. Proportions of these rock types vary greatly, both across the exposed belt and parallel to it (Standlee 1978b, Varga 1980, Bond & Devay 1980), although tuffs appear to be more abundant in the easternmost, presumably younger parts of the complex (Clark & Huber 1975, Standlee 1978b, Varga 1980). The rocks in most exposures are penetratively deformed, contain lower greenschist facies alteration assemblages, and have quartz textures indicative of syntectonic recrystallization. The Shoo Fly complex is known to be entirely pre-Late Devonian (Anderson *et al.* 1974, Durrell & D'Allura 1977, Devay & Stanley 1979) and parts of the complex contain fossils of Ordovician/Silurian age (D'Allura *et al.* 1977, Varga & Moores 1981).

Provenance and facies analysis of sandstones within the Shoo Fly complex suggest deposition adjacent to a passive continental margin (Bond & Devay 1980), which some authors suggest was the early Paleozoic North American margin (D'Allura *et al.* 1977, Bond & Devay 1980, Schweickert & Snyder 1981, Varga & Moores 1981, Varga 1982, Girty & Wardlaw 1984). Serpentinite-matrix mélange occurs discontinuously along the eastern contact of the complex where it is unconformably overlain by Late Devonian volcanic rocks (Schweickert 1974). The significance of this eastern mélange belt has been discussed in terms of implications for mid-Paleozoic tectonics of the region (Schweickert & Snyder 1981, Varga & Moores 1981).

MESOSCOPIC STRUCTURAL FABRIC OF THE SHOO FLY COMPLEX

The mesoscopic structural fabric of the Shoo Fly complex was defined along four major river courses

which drain the northern Sierra Nevada (Fig. 2). These rivers, the North Fork of the Feather River, the East Branch of the North Fork of the Feather River, the Middle Fork of the Feather River, and the North Fork of the Yuba River, are referred to in this paper as Traverses I–IV, respectively. In addition to these four traverses, a glaciated and well-exposed area in the Lakes Basin region (Fig. 2) was mapped and studied in detail.

Three periods, or phases, of deformation and folding were noted in the Shoo Fly complex, although not all fold phases are represented in each of the five domains studied. Structures produced during each period of deformation are described in detail below in order of formation, with special attention paid to structures thought to reflect Nevadan deformation.

Pre-Nevadan Structures (F1)

Folds which predate penetrative cleavage in the Shoo Fly complex were found at two localities during this study (Traverse IV and Lakes Basin region), but may have been widespread prior to later intense Nevadan deformation. *F*1 folds have many geometric similarities to later-formed Nevadan folds but are recognized where they are crosscut by Nevadan cleavage or are deformed into complex interference patterns.

Figure 3(a) shows an outcrop example of a small-scale *F*1 fold. Larger-scale *F*1 folds have been discerned through plane table mapping in the Lakes Basin region (discussed below). Folds of this generation typically have close to isoclinal interlimb angles (Fig. 4a & d) and high-amplitude fold surface form with variable shape (Figs. 4b & e). Orthogonal thickness analysis of *F*1 fold layers shows them to be largely intermediate between ideal parallel (class 1B) and ideal similar (class 2) folds (Figs. 4c & f). Some of the irregularity in *F*1 fold profile geometry is due to later deformation.

Presence of metamorphic cleavage parallel to the axial surfaces of *F*1 folds cannot be convincingly demonstrated from results of this study. Thin sections cut perpendicular to the axes of several small *F*1 folds show a faint alignment of phyllosilicates parallel to some *F*1 axial surfaces. However, such alignment may well be an inherited sedimentary fabric due to an original alignment of platy minerals parallel to bedding. Support for a tectonic origin for an *F*1-related cleavage was documented by Russell (1977), who observed recrystallized quartz and feldspar parallel to the axial surfaces of *F*1 folds in the area of Traverse IV.

Axes of *F*1 folds lie along a great-circle oriented N38°W, 73°NE (Fig. 5a) and have axial surfaces with poles which lie along a NNE-striking great-circle (Fig. 5b). As discussed below, the great-circle distribution of *F*1 fold axes may be largely due to rotation toward the extension axis operative during Nevadan deformation.

Development of *F*1 folds predates deposition of Late Devonian volcanics which overlie the Shoo Fly complex throughout the northern Sierra Nevada and may be related to collision and subduction at the mid-Paleozoic Cordilleran margin (Schweickert & Snyder 1981, Varga & Moores 1981, Schweickert 1981).

Nevadan Structures (F2, F3)

Throughout the Sierra Nevada intense mid-Mesozoic deformation produced a variety of structures which control the present northwest disposition of lithologies in the range (Fig. 1). In the northern Sierra Nevada, two distinct phases of deformation are recognized as a result of this Nevadan event. The first phase (*F*2) formed penetrative cleavage, isoclinal folds, and associated lineations which dominate the fabric of Late Jurassic and older rocks throughout the region. The second phase (*F*3) formed kink folds and a crenulation cleavage which are non-penetrative, discontinuously developed, and variably oriented. Regional, low-greenschist facies metamorphism accompanied formation of *F*2-related cleavage.

F2 *Structures*

Nevadan folds with well-developed axial-planar cleavage were observed at all localities studied (Figs. 3b & c). The folds are tight to isoclinal (Figs. 6a, d, g, j & m) and have nearly ideal class 2 layer thickness form (Figs. 6c, f, i, l & o). Fold surface form is variable and somewhat dependent on lithology in each area but can be characterized as subrounded to angular and of high amplitude (Figs. 6b, e, h, k & n). Lineations, which commonly parallel local axes of *F*2 folds, include small crenulation axes (Fig. 3d), slickensides, quartz boudin axes, and bedding/cleavage intersections. Cleavage (*S*) is defined by parallel alignment of phyllosilicate minerals, dominantly muscovite, in fine-grained rocks and by discrete fracture surfaces in sandstone. Cleavage fans are common in the axial portions of folds where *S* refracts from fine-grained to coarse-grained lithologies (Fig. 3c).

Orientation of *F*2 structures is shown for each area in Fig. 2. *F*2 fold axes lie within well-defined, NNW-trending great-circle girdles which parallel *S* in each area (along Traverse II, a contiguous area of Shoo Fly complex contains *F*2 structures with WNW orientations due to rotation by large-scale *F*3 folds. *F*2 structures in this particular area have been restored to pre-*F*3 orientations, as defined by unrotated structures in surrounding regions, and plotted stereographically in Fig. 2). In all areas except the Lakes Basin region, axes of *F*2 folds are strongly concentrated about maxima which plunge steeply to the NNW. Axes of *F*2 folds from all areas are plotted in Fig. 5(d) and define a NNW-trending great-circle with a well-defined maximum oriented 82°N14°W.

F3 *Structures*

'Kink' folding of the more intensely foliated, fine-grained portions of the Shoo Fly complex followed generation of *F*2 isoclinal folds. The folds vary in style from isolated kink flexures (Fig. 7a), to conjugate fold

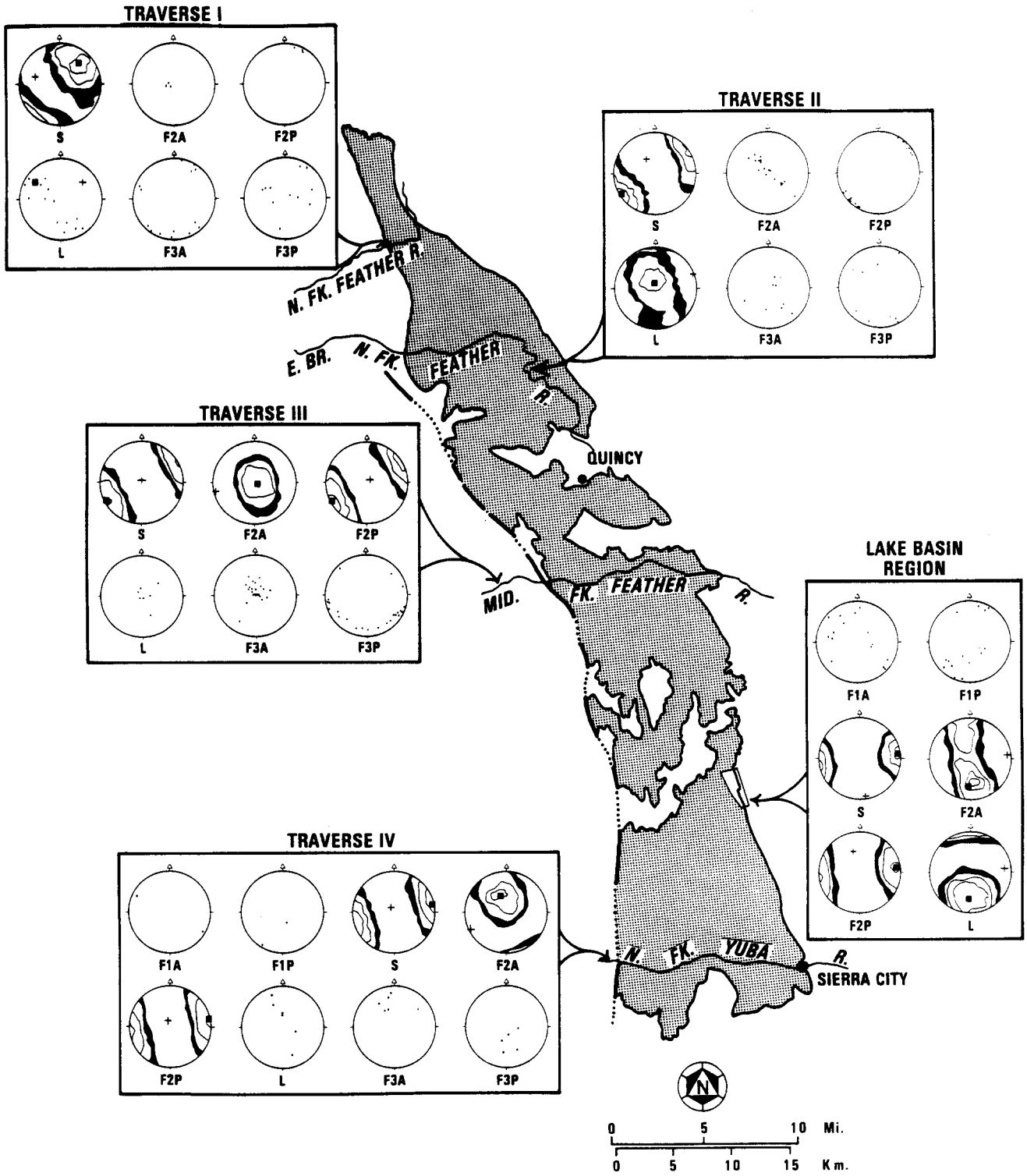

Fig. 2. Stereoplots showing mesoscopic structural data from five domains within the Shoo Fly complex. Stippled pattern is generalized outcrop area of the complex. Town names index the map to Fig. 1. Lakes Basin region is shown as box along eastern edge of contact, immediately north of Traverse IV. *S*, cleavage; *F1A*, axes of pre-Nevadan folds; *F1P*, poles to axial planes of pre-Nevadan folds; *F2A*, axes of main phase Nevadan folds; *F2P*, poles to axial planes of main phase Nevadan folds; *L*, lineations related to *F2* folds; *F3A*, axes of Late Nevadan folds; *F3P*, poles to axial planes of Late Nevadan folds. Stereoplots contoured in multiples of standard deviation from an assumed random distribution (Kamb 1959). Shaded areas of stereonets lie between 2σ and 4σ contour intervals and contain expected number of data points, assuming a random distribution. +, pole to best-fit plane through data; ■, best-fit axis through data as calculated by eigenvector analysis (Darot & Bouchez 1976). See Appendix for statistics of plots.

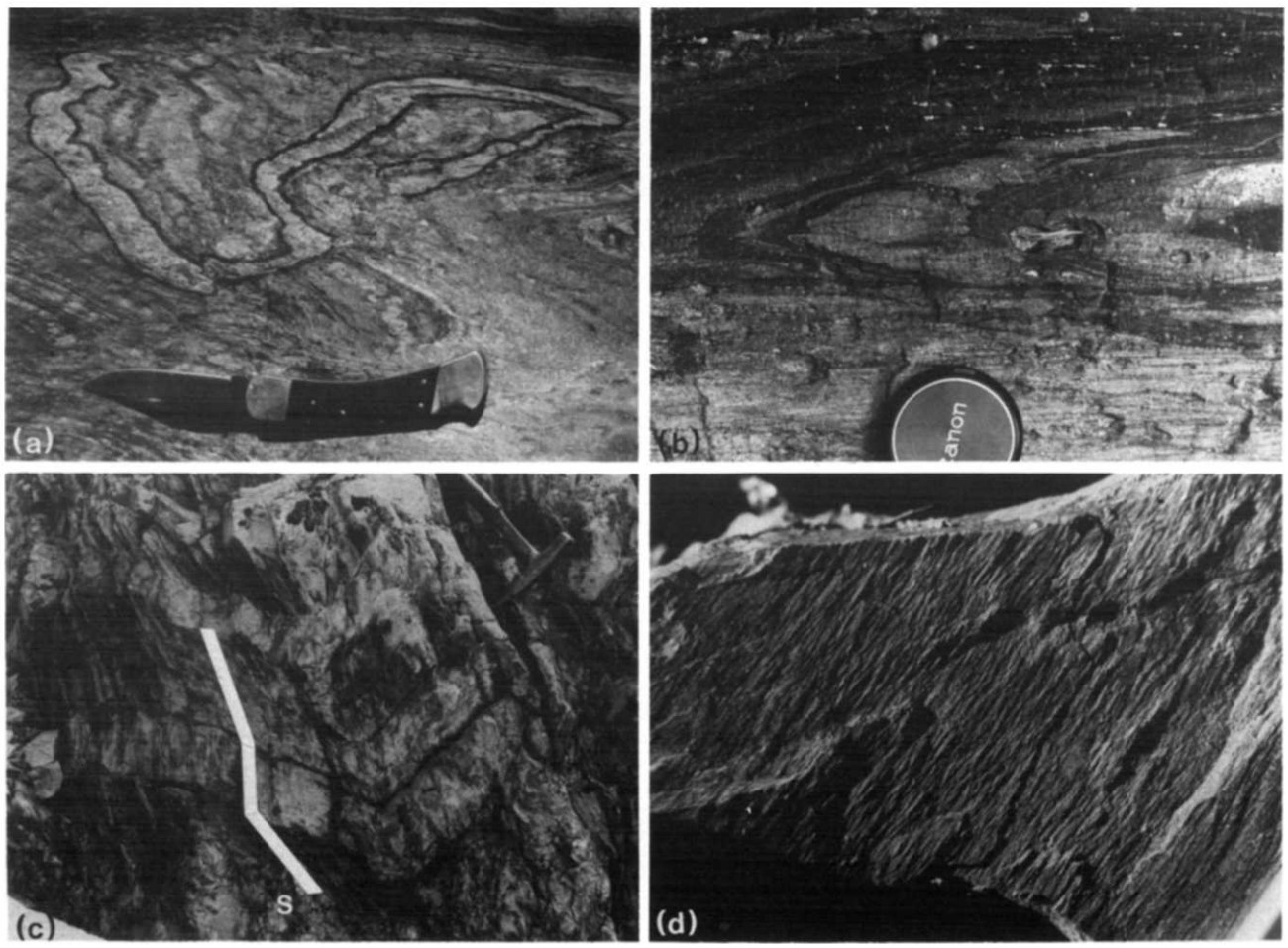

Fig. 3. (a) *F*1 folds in siltstone and shale units along Traverse IV crosscut and folded by Nevadan structures (*S* is parallel to knife). Note apparent type 3 (Ramsay 1967) interference structure. (b) Nearly ideal class 2 (Ramsay 1967) *F*2 fold along Traverse III in shale unit. (c) Class 1B to 1C fold in tuffaceous rocks in Lakes Basin region. Note refraction of *S*. (d) Crenulations parallel to *F*2 axis along Traverse IV.

Fig. 7. (a) *F*3 'kink' fold in shale along Traverse I. (b) *F*3 folds from Traverse III with incipient axial-planar cleavage (parallel to pencil). Note *F*2 hinge areas (arrows).

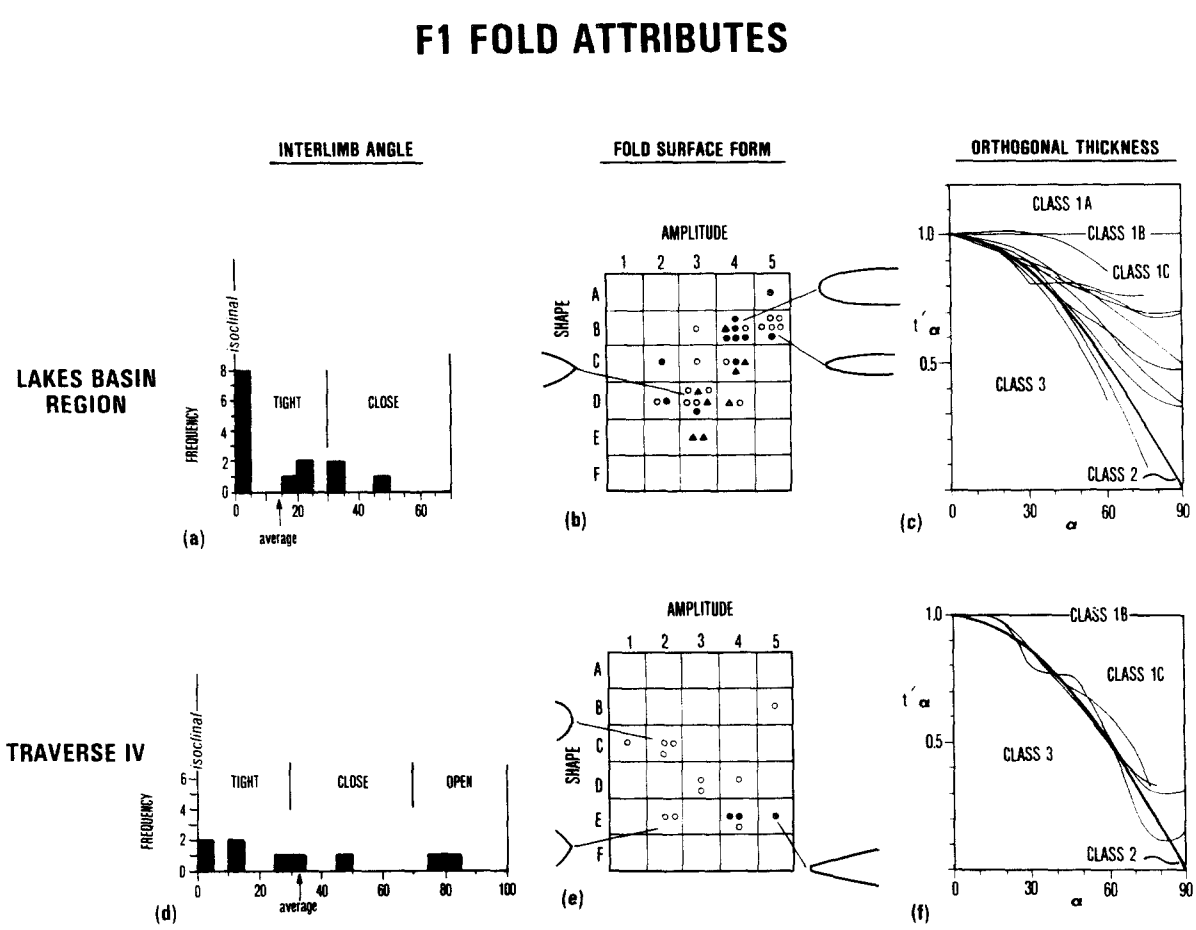

Fig. 4. Geometric attributes of $F1$ folds. Methods used in construction of interlimb angle, fold surface form, and orthogonal thickness diagrams are contained in Fleuty (1964), Hudleston (1973a) and Ramsay (1967), respectively. Symbols in (b) and (e) are, o, sandstone; ●, shale and siltstone; ▲, chert.

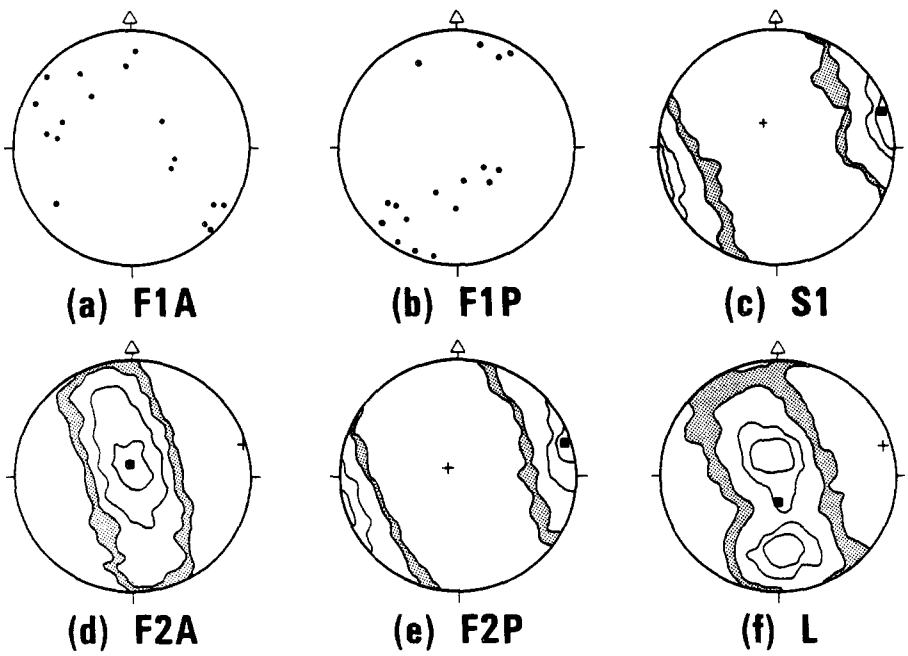

Fig. 5. Synoptic stereoplots of data from all domains. See Fig. 2 for discussion of symbols and Appendix for statistics.

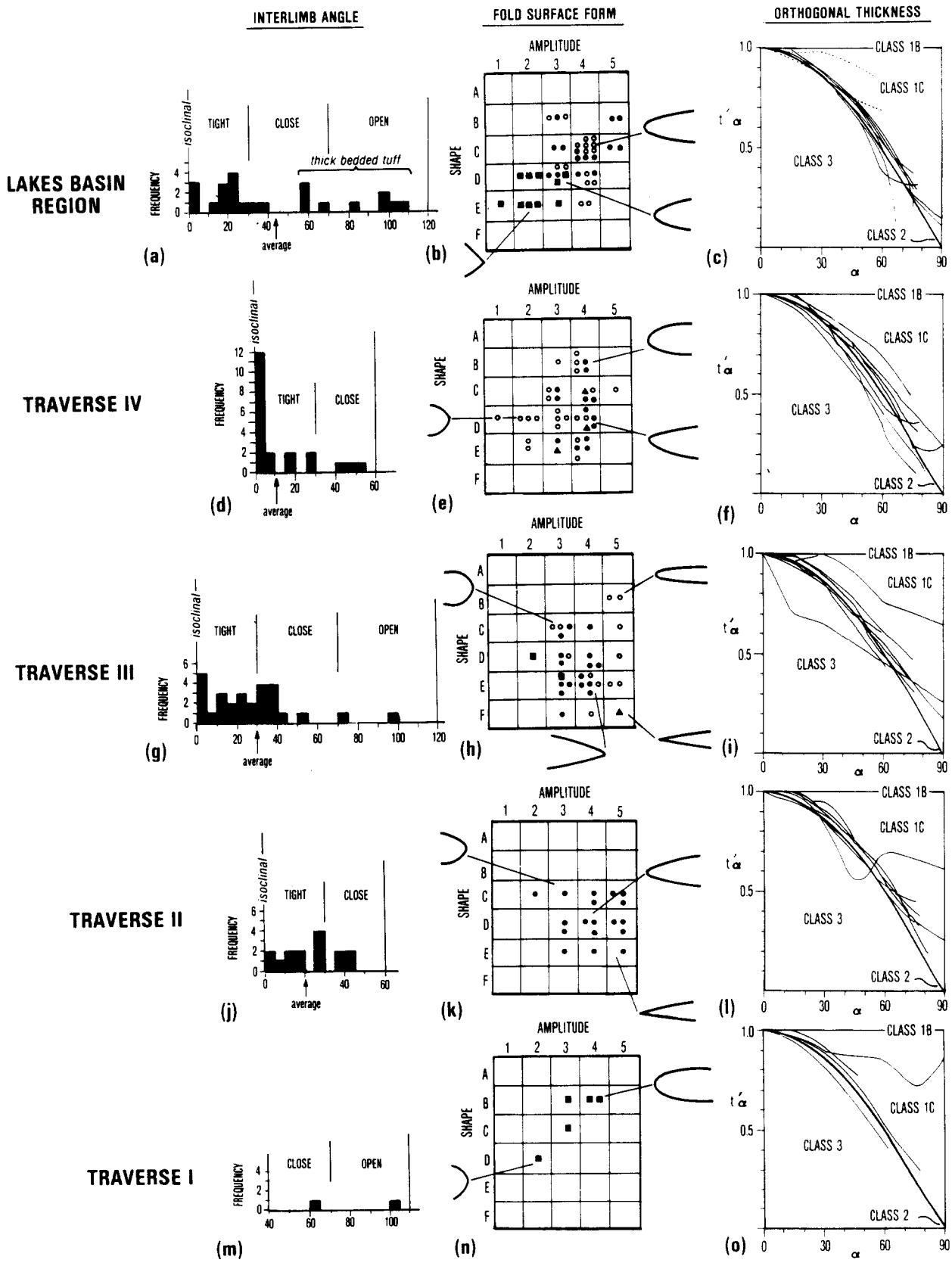

Fig. 6. Geometric attributes of $F2$ folds. Symbols for fold surface form are the same as in Fig. 4 but ■, thick-bedded tuffaceous sandstone in Lakes Basin region and limestone in Traverses III and IV.

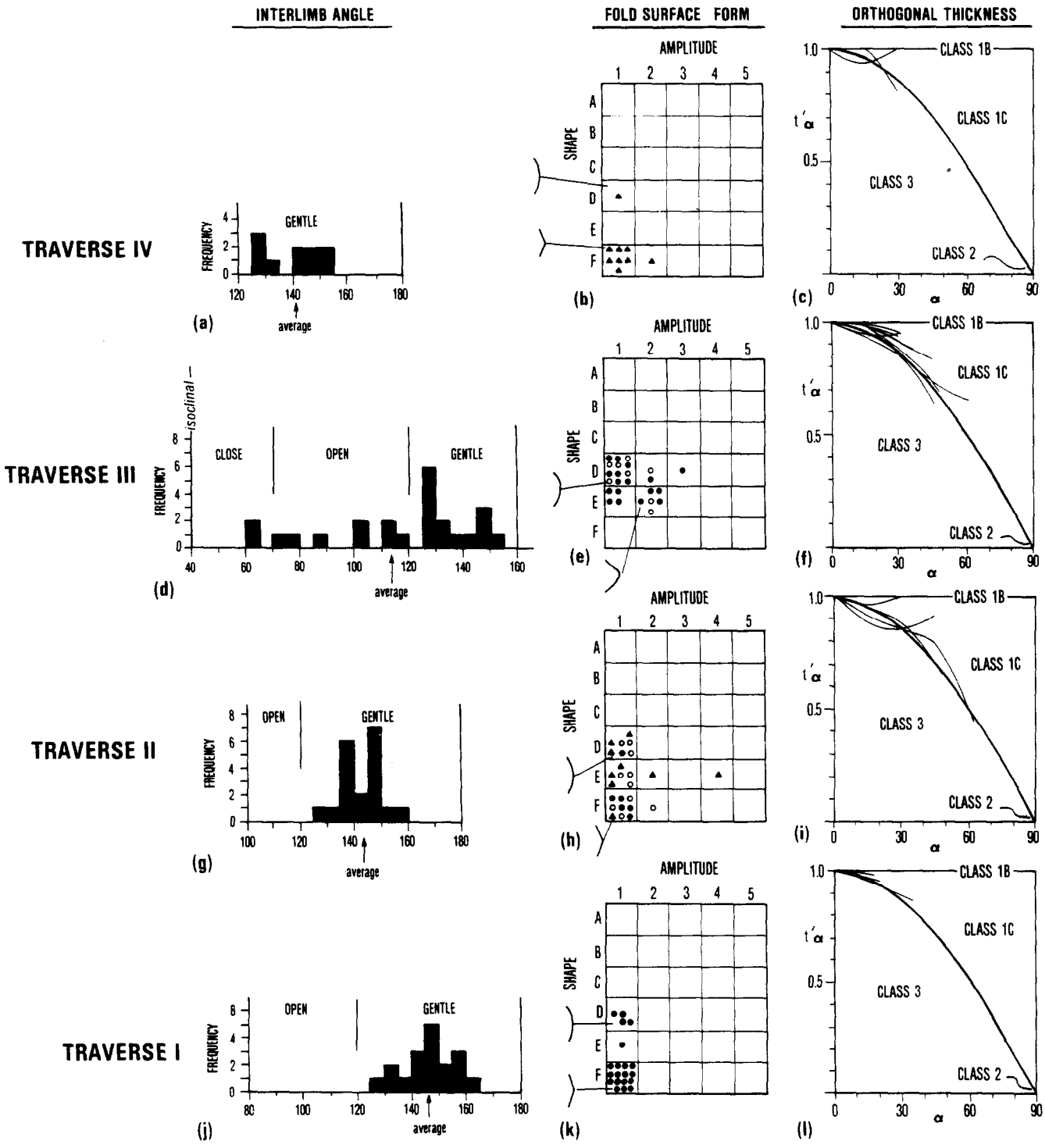

Fig. 8. Geometric attributes of $F3$ folds. Symbols for fold surface form are the same as in Fig. 4.

pairs, to nearly similar folds with incipient axial-planar cleavage (Fig. 7b). Large-scale $F3$ folds, with wavelengths up to 3 km, occur along Traverse II. Although $F3$ folds have many features of classical kink flexures, such as open to gentle interlimb angles (Figs. 8a, d, g & j) and sharp hinge areas (Figs. 8b, e, h & k), most of the folds examined in detail possess hinge zone thickening and 'similar' geometry (Figs. 8c, f, i & l).

The orientation and asymmetry of $F3$ structures varies considerably between each area of this study (Fig. 2) and, thus, few generalizations can be made regarding the significance of this period of deformation. The lack of consistency in orientation, form and pervasiveness of $F3$ structures probably reflects, in part, the low total finite strain of this deformation.

Timing of F2 *and* F3 *Structures*

Several lines of evidence indicate that $F2$ structures are definitely the result of Mesozoic deformation and, further, were probably produced during the Late Jurassic Nevadan orogeny. Immediately east of Traverse II, slaty cleavage and isoclinal folds with orientations parallel to $F2$ structures in the Shoo Fly complex cut rocks as young as Callovian (McMath 1966). East of Sierra City (Fig. 2) the Haypress Creek pluton (154 Ma) cuts Jurassic or older strata with a similar cleavage (Schweickert *et al.* 1984). Thus, $F2$ deformation occurred sometime in the Late Jurassic. In support of a Late Jurassic age for this deformation are paleomagnetic data from Permian rocks in the area around Traverse II, which suggest remagnetization during metamorphism and cleavage formation at about 150 Ma (Hannah & Verosub 1980).

Timing of $F3$ structures is problematic because of their non-penetrative, domainal occurrence coupled with the lack of post-Late Jurassic Mesozoic strata in the region which would likely record such low strain deformation. Schweickert *et al.* (1984) have shown that N20–30°E-trending, domainal, spaced to slaty cleavages and associated folds in the Sierra City region (Fig. 2) are cut by the late Jurassic Haypress Creek pluton and are, thus, 'late' Nevadan in age. While many of the $F3$ structures measured during this study (Fig. 2) are parallel to those dated by Schweickert *et al.* (1984), many are not. However, careful structural and geochronological work in the central Sierra Nevada (Tobisch & Fiske 1976, 1982) has shown that development of 'kink-style' folds and crenulations closely follows development of each discrete period of mid- to late-Mesozoic slaty cleavage. In this view, these late folds formed during the waning phases of a continuum of deformation which records the change from relatively ductile (formation of slaty cleavage) to relatively brittle (formation of crenulations and kinks) conditions. The morphology of $F3$ folds described in this study supports a similar interpretation. Incipient slaty cleavage in the hinge areas of some $F3$ folds (Fig. 7b) and their commonly 'similar' layer thickness geometry (Figs. 8c, f, i & l) both suggest that the rocks were somewhat ductile during deformation but were sufficiently brittle to produce folds with long limbs and sharp, angular hinge areas. Thus, $F3$ folds can be envisioned as forming shortly after $F2$ structures and under somewhat lower grade metamorphic conditions.

In summary, both $F2$ and $F3$ structures of the northern Sierra Nevada are considered to have formed during the Nevadan orogeny, probably during latest Jurassic time. It is realized that in areas of the Sierra Nevada to the south of the region discussed here, structures which lie parallel to the 'typical' Nevadan trend (NNW) may have formed from Late Jurassic to at least mid-Cretaceous time (Tobisch & Fiske 1982). Other authors argue for early Mesozoic deformations about NNW trends (e.g. Saleeby 1977, 1981, Kistler 1966, Russell & Nokleberg 1977), although timing of these earlier events is controversial (Schweickert 1981). The view favored here, of a short-lived Late Jurassic (possibly into the Cretaceous) deformation for the northern Sierra Nevada is supported by geological relations in terranes to the west of the Shoo Fly complex (Smartville complex and Central belt) which record an abrupt arc-continent collision (Moores & Day 1984) closely dated at about 155 Ma (Schweickert *et al.* 1984).

KINEMATICS OF NEVADAN DEFORMATION

Tectonic models for Nevadan deformation in the Sierra Nevada are generally partially based on interpretation of well-known large-scale features of the orogen, such as the Foothills fault system. Nevadan structures are typically considered to be W-vergent (e.g. Davis 1969), although folds and thrusts are interpreted to be E-vergent in the northern part of the range (Moores & Day 1984). However, in considering whether Nevadan deformation was caused primarily by transpression (Saleeby 1977, 1978, 1981, Burchfiel & Davis 1981) or by compression at nearly right angles to the axis of the Sierra Nevada (Schweickert & Cowan 1975, Schweickert 1981, Moores & Day 1984), these non-penetrative, relatively high-level structures might be regarded as non-diagnostic, as such structures can form in both dominantly compressional (e.g. Canadian Rocky Mtns) or dominantly transpressive (e.g. Transverse Ranges portion of the San Andreas Fault system) regimes. In contrast, the Shoo Fly complex occupied the deep-seated core of Eastern belt (Fig. 1) rocks during the Nevadan orogeny and, in the northern Sierra Nevada, was deformed dominantly by penetrative ductile flow. As discussed below, these ductile structures are believed to be sensitive indicators of Nevadan kinematics at depth and, by inference, of causative Late Jurassic plate dynamics.

Main phase ($F2$) Nevadan structures of the Shoo Fly complex are analyzed below in an attempt to place constraints on the orientation of the bulk finite strain ellipsoid associated with Nevadan deformation. The resulting orientations are compared to 'slip line' determinations constructed through analysis of the effects of $F2$ structures overprinting $F1$ folds.

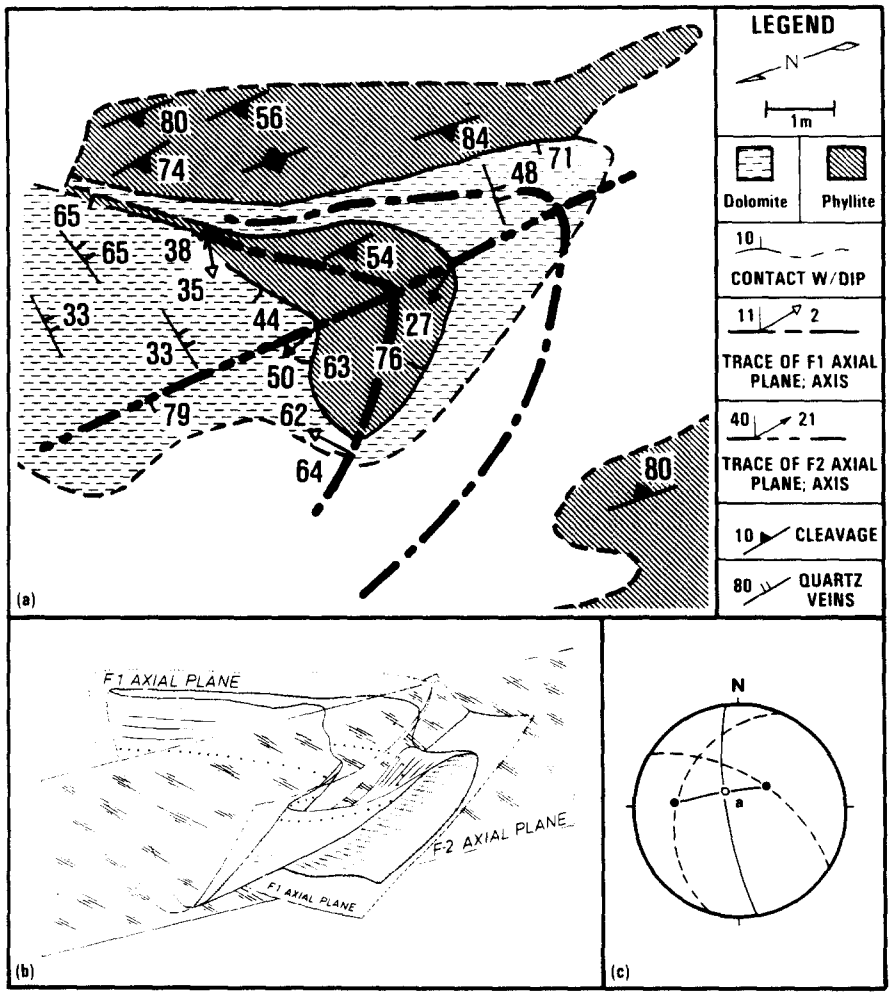

Fig. 9. (a) Plane-table map of type 2 interference fold pattern in Lakes Basin region where an $F2$ fold crosscuts $F1$ folds. (b) Three-dimensional reconstruction of contact between phyllite and dolomite units. (c) Stereoplot showing construction of extension direction a operative during $F2$ deformation. Solid dots are $F1$ measured at apices of interference 'arrow'. Dashed lines are $F1$ surfaces, solid great-circle is S. See text for discussion of construction method.

Formation of F2 *Structures*

Orthogonal thickness relations of $F2$ folds (Figs. 6c, f, i, l & o) show that most folds of this generation possess nearly ideal class 2, or 'similar' geometry. Many authors have noted how similar folds can begin as parallel, or concentric, buckles (class 1B) and attain similar geometry through simultaneous, or later, homogeneous flattening (Flinn 1962, Mukhopadhyay 1965, Ramsay 1967, Hudleston & Stephansson 1973, Hudleston 1973a). In these models, class 2 geometry is approached by extreme flattening ($\lambda_1/\lambda_2 \rightarrow \infty$). Similar folds can also form in simple shear regimes (Cobbold & Quinquis 1980) or through a combination of simple shear and homogeneous flattening (Matthews *et al.* 1971).

Although the various models for similar folding suggest important mechanical and kinematic differences, the resultant geometries are comparable for large strains. Of importance for this discussion are that all models predict that material lines will tend to rotate toward the X axis of the finite strain ellipsoid ($X > Y > Z$) and that, for large strains, axial-planar cleavage will approximate the XY plane, in accordance with field observations (Wood 1974). Considerable shearing along cleavage planes can, however, occur during deformation if early formed cleavage traces deviate even slightly from the XY plane (Ghosh 1982).

Nearly ideal class 2 geometry of most $F2$ folds in the Shoo Fly complex, the presence of some $F2$ folds with class 1B to 1C geometry, and the lack of consistent asymmetry suggest that $F2$ folds were formed by a combination of buckling and a large component of flattening strain. Axes of all $F2$ folds form a well-defined girdle (N16°W, 87°SW, Fig. 5d) which lies approximately parallel to the regional slaty cleavage (Fig. 5c). The locus of fold axes contains a distinct maximum which plunges steeply NW. The steep maximum of $F2$ fold axes is believed to be due to near-vertical extension during Nevadan deformation and not to simple intersection of steep $F2$ axial surfaces (and cleavage) with pre-existing steep bedding orientations within the Shoo Fly complex. Figure 5(b) shows that many $F1$ folds have axial surfaces which are gently to moderately dipping. Where exposure permits examination of the superposition of $F1$ and $F2$ structures (Fig. 9), $F1$ axial surfaces are observed to have been originally moderately to gently dipping and rotated into steeper orientation by $F2$ deformation. Thus, $F1$ folds were generally reclined to recumbent prior to Nevadan deformation. Near-vertical extension is also evidenced locally by gently dipping

quartz veins that are perpendicular to $F2$ fold axes.

Following Flinn (1962) and considering fold axes as material lines which rotate during progressive deformation, the $F2$ axis maximum is taken to approximate the X axis of the bulk finite strain ellipsoid. Assuming the synoptic S-plane to approximate the XY plane, yields a finite strain ellipsoid, the axes of which approximate the following directions: X = 82°N14°W ($F2$ axis maximum), Y = 8°S20°E, Z = 6°N71°E (pole to synoptic S-plane).

F2/F1 *Interference structures*

Where $F1$ folds have been observed in the field, they invariably are deformed by $F2$ structures into shapes comparable to those depicted by Ramsay (1967) and discussed recently by Thiessen & Means (1981). In two areas of the Lakes Basin region, deformed $F1$ folds were sufficiently exposed in three dimensions to permit analysis of their geometry and to allow construction of a 'slip line', or extension direction related to $F2$ deformation.

Figure 9(a) is a plane table map of a complexly folded area in the Lakes Basin region in which the contact between a carbonate unit and a phyllite unit define an arrowhead shape identical to Ramsay's (1967) type 2 interference structure. A diagrammatic, three-dimensional reconstruction of this structure is shown in Fig. 9(b). The deformed $F1$ hinge lines can be treated as a lineation deformed by similar style folding using the classical methods of Weiss (1959) and Ramsay (1967). Hudleston (1973b) demonstrated that application of the Weiss–Ramsay construction to lineations deformed by simultaneous buckling and flattening may result in derivation of the extension direction for second folding. Applying this construction to the fold in Fig. 9, and assuming that the $F1$ axes measured at the apices of the interference structure represent opposite ends of an originally rectilinear $F1$ axis, yields an extension direction for $F2$ deformation of 70°N37°W.

The extension direction derived for a second $F2/F1$ interference structure mapped in detail within the Lakes Basin region is shown in Fig. 10. Also shown on Fig. 10 is the extension direction derived by considering the planar distribution of $F1$ fold axes measured throughout the northern Sierra Nevada (Fig. 5a) as the locus of a lineation rotated by $F2$ deformation.

The extension directions derived through analysis of $F2/F1$ interference relationships plunge steeply NW and lie close to the extension direction defined by the $F2$ fold axis maximum (Fig. 10). The steeper plunge of the $F2$ axis maximum is, however, considered to more closely reflect the integrated regional extension axis, as it was derived using data from throughout the area. Thus, deep basement rocks of the northern Sierra Nevada responded to main phase Nevadan compression by nearly vertical, penetrative ductile flow. At high structural levels compression was accommodated by horizontal movement along discrete thrust faults and by formation of large, overturned folds.

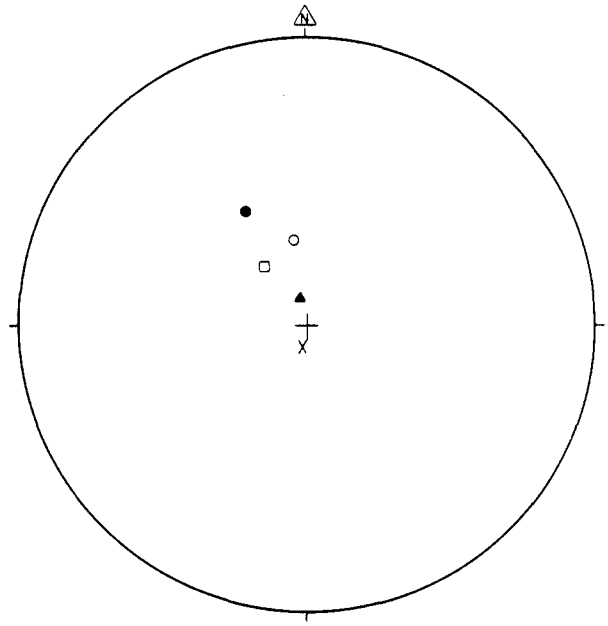

Fig. 10. Stereoplot showing extension direction for main phase Nevadan deformation derived by (1) mapping of individual $F2/F1$ interference structures (o, □ = fold in Fig. 9), (2) rotation of all $F1$ axes toward a common $F2$ extension direction (●), (3) $F2$ fold axis maximum (▲). X, Nevadan extension direction derived by Tobisch & Fiske (1982).

RELATIONSHIP OF NEVADAN FABRICS TO JURASSIC PLATE KINEMATICS

Main phase Nevadan deformation

The extent to which a mesoscopic structural fabric can be related to regional plate dynamics depends upon the areal pervasiveness of the fabric and the degree to which the fabric reflects the complete kinematic framework; i.e. does the fabric record both the vertical and horizontal components of plate motion? Clearly, regionally developed penetrative ductile fabrics can be sensitive indicators of relative plate motion because they reflect plastic flow within rocks in which layering and other anisotropies have deformed relatively passively. Ductile fabrics have been used to infer a variety of relative plate motions in orogens ranging from orthogonal (Escher & Watterson 1974, Shackleton & Ries 1984, Karlstrom & Houston 1984), to transform (Coward *et al.* 1973, Nicolas *et al.* 1977, Shackleton & Ries 1984), to oblique or 'transpressive' (Harland 1971, Nicolas & Boudier 1975, Boudier 1978, Sibson *et al.* 1981) convergence.

The main phase ($F2$) Nevadan fabric within the Shoo Fly complex of the northern Sierra Nevada has a consistent orientation over the area studied and may be consistent with similar age fabrics elsewhere in the range. The relatively uniform NNW trend of Nevadan structures along the length of the Sierra Nevada has been emphasized by a number of authors and summarized recently by Schweickert (1981) and Schweickert *et al.* (1984). However, strain directions for Nevadan deformation have been assessed at very few localities. In a detailed study of the Ritter Range roof pendant of the

central Sierra Nevada, Tobisch *et al.* (1977) and Tobisch & Fiske (1982) established an essentially vertical extension direction for Nevadan deformation within a NNW flattening foliation (Fig. 10). Best (1963) and Paterson & Redfield (1984) derived similar strain axis directions for Jurassic volcanic rocks of the southwestern Sierra Nevada. Down-dip lineations of presumed extension origin are common within NNW-trending cleavages elsewhere in the Sierra Nevada (Saleeby 1981), but the age and kinematic significance of these particular structures are uncertain. Thus, principal directions of finite strain of main phase Nevadan structures within the northern Sierra Nevada are nearly coaxial with those derived from rocks over 300 km to the south and are consistent with structures along much of the length of the range.

Penetrative ductile fabrics within metamorphic rocks of the Sierra Nevada suggest ENE flattening and nearly vertical material flow during the Nevadan orogeny. This general strain pattern is consistent with essentially orthogonal compression at right angles to the length of the range and is also consistent with orthogonal convergence of the Sierran margin with accreted oceanic and/or island arc terranes. Thus, the Nevadan strain data support two-dimensional plate models (Moores 1970, Schweickert & Cowan 1975, Schweickert 1981, Moores & Day 1984).

Saleeby (1977, 1978, 1981) suggested a holistic model for Mesozoic deformation of the Sierra Nevada wherein the western edge of the range is a dextral transform fault(s) which separated the developing Sierran arc from oceanic terranes to the west. Material was accreted along the transform margin as subduction stepped progressively westward. Deformation of the arc and its wallrocks occurred throughout much of the mid-Mesozoic in response to oblique convergence and resultant transpression. The Late Jurassic Nevadan orogeny, in this model, is viewed as a particularly intense pulse of transpression during a relatively protracted deformation.

In his model for Nevadan deformation, Saleeby (1981) acknowledged the vertical extension direction for metamorphic rocks of the Sierra Nevada but suggested that they represent only the compressive component of transpression and that the horizontal component was dissipated along major, intra-arc transcurrent faults represented by the present Foothills fault system (Clark, 1960). As a modern analog, Saleeby (1981) suggested the Semangko fault zone of Sumatra, a major dextral, intra-arc transcurrent fault zone. Motion along this zone is sympathetic to oblique convergence of the Sunda Arc with the Indian Ocean plate.

Available field data from examples cited below do not support the concept of Saleeby (1981) that the horizontal component of transpressive continental margins is dissipated along discrete transcurrent faults, whereas the compressive component is dissipated within a wider belt of deformation. Harland (1971), who coined the term 'transpression', stated that positive evidence for oblique plate convergence and associated deformation are extension structures parallel to the orogen. The type transpressive margin described by Harland is the NS-trending western portion of Spitsbergen Island, in which Caledonian-age oblique convergence produced a variety of ductile fabrics including foliation, boudinage and stretched pebble conglomerates (Weiss 1953, Harland 1971). These fabrics suggest significant extension parallel to the deformed margin. Other regions in which extensional ductile fabrics faithfully reflect the kinematics of transpression include the Alpine fault zone in New Zealand (Sibson *et al.* 1981), the Ivrea Zone in the western Alps (Boudier 1978, Nicolas & Boudier 1975), the Armorican belt (Nicolas *et al.* 1977), and the Mayden zone in Afghanistan (Nicolas *et al.* 1977). Conversely, in regions of orthogonal plate convergence extension directions are nearly perpendicular to plate boundaries. Examples include the northern Himalayas and southern Tibet, the Caledonides of the British Isles and Scandinavia, and the Mozambique belt (Shackleton & Ries 1984), and the Cheyenne Belt in Wyoming (Karlstrom & Houston 1984).

Further support for an essentially two-dimensional, compressive deformation for the Nevadan orogeny comes from recent work on the sense of displacement along faults of the Foothills fault system in the northern Sierra Nevada. The sense of displacement along faults of this system has historically been difficult to document, which has led to a variety of kinematic scenarios being offered (see discussion in Saleeby 1981). However, detailed structural and petrofabric studies by Russell (1977) and Tuminas (1983) on strands of the zone in the northern Sierra Nevada strongly suggest that the faults experienced dominantly dip-slip movement. The major faults of this zone, such as the Melones fault zone, have recently been interpreted as E-directed thrust faults which have subsequently been steepened by W-directed backfolding (Moores & Day 1984). Down-dip stretching lineations within the Melones fault zone south of the area shown in Fig. 1 (Schweickert *et al.* 1984) suggest that orthogonal convergence during the Nevadan orogeny was important along much of the length of the Sierra Nevada.

In summary, the penetrative fabrics of the Shoo Fly complex and of faults of the Foothills fault system provide a mutually consistent kinematic framework for deformation during the main phase of the Late Jurassic Nevadan orogeny in the northern Sierra Nevada. Compression perpendicular to the orogen, probably due to emplacement of the Smartville Complex (Schweickert & Cowan 1975, Moores & Day 1984) caused development of E-directed thrust faults and E-vergent folds. Basement rocks in the Eastern belt (Shoo Fly complex) responded to compression by near-vertical ductile flow. If transcurrent motion was important along the margin during this time period, as suggested by Saleeby (1977, 1978, 1981) for the southern Sierra Nevada, it did not impart a discernible fabric to the northern portion of the range.

Late stage Nevadan structures

The significance of $F3$ structures, which were pro-

duced during the waning phases of the Nevadan orogeny, is unclear in the northern Sierra Nevada because of the lack of consistency in style and orientation of these structures across the region and the uncertainty as to their age from area to area (Schweickert *et al.* 1984). Tobisch & Fiske (1976) suggested that similar structures in the central Sierra Nevada could be related to 'elastic recovery' following the main phase of the Nevadan orogeny during which time relaxation of compressive stress caused a small amount of shortening parallel to the length of the orogen. Alternative causes of late kinking might include slight reorientation in the relative motion between the Sierra Nevada and colliding oceanic plates, minor NW–SE compression due to margin irregularity during collision, or back-thrusting and folding. Of these models, the concept of late Nevadan back-thrusting and folding is attractive because of the field evidence for it (Moores & Day 1984). Such an Alpine-type 'rotation' event (Roeder 1973) might explain the horizontal to moderately plunging *F*3 folds found along Traverses I and IV (Fig. 2) but fails to explain steeply plunging *F*3 folds, such as those found along Traverses II and III as well as those described by Tobisch & Fiske (1976).

As pointed out by Anderson (1968) and Gay & Weiss (1974), '*F*3-type' deformation in mountain belts typically involves only a few percent shortening, which is in strong contrast to the extreme shortening related to the main phase Nevadan cleavage-forming event (Tobisch & Fiske 1982). This relative 'ease' of kink folding, coupled with the inherent complexities in geometry and history of collisional margins, make it likely that *F*3-type structures might have quite different causes, if not ages, in different parts of the Sierra Nevada and that a unifying model for their origin will remain elusive.

CONCLUSIONS

Late Jurassic near-vertical extension within early Paleozoic basement rocks of the northern Sierra Nevada was synchronous with formation of E-directed thrust faults and macroscopic folds in younger rocks of the Eastern belt and in exotic Mesozoic rocks west of the Feather River Peridotite belt. The penetrative main phase Nevadan structures in early Paleozoic rocks of the Eastern belt are interpreted as indicators of the relative motion of the belt with the Smartville Complex and related rocks during their emplacement against the western margin of North America in the Late Jurassic. This interpretation suggests dominantly orthogonal convergence between the continental margin and the island arc-ophiolite terranes.

Orthogonal convergence between terranes in the northern Sierra Nevada contrasts with a model suggested by Saleeby (1977, 1978, 1981), in which accretion and deformation is accomplished in a transpressive regime related to dextral transform fault motion along the North American margin. Review of the structural fabric of transform/transpressive margins in other areas shows that the transcurrent and compressive components of motion between lithospheric plates are expressed both within fault zones and within wider belts of deformation. Transpressive margins invariably possess structures which suggest a large component of axial elongation. The near-vertical extension direction derived here, coupled with recent evidence which suggests dip-slip motion on fault zones related to terrane accretion, argues against a significant strike-slip component to Nevadan deformation in the northern Sierra Nevada.

Acknowledgements—This study was undertaken while the author was a student at University of California at Davis and was supported by NSF grant EAR 76-14270. I thank E. Moores, R. Twiss, G. Bond and R. Schweickert for discussions of this work and E. Moores, R. Schweickert and R. Hickman for reviews of an earlier manuscript. Comments by two anonymous reviewers proved most useful. Support for manuscript preparation by Union Oil Company of California and the drafting of figures by C. Reis and A. Addy are gratefully acknowledged.

REFERENCES

Anderson, T. B. 1968. The geometry of a natural orthorhombic system of kink bands. In: *Kink Bands and Brittle Deformation* (edited by Baer, A. and Norris, D.) *Geol. Surv. Pap. Can.* **68–52**, 200–220.

Anderson, T. B., Woodward, G. D., Strathouse, S. M. & Twitchell, M. K. 1974. Geology of a Late Devonian fossil locality in the Sierra Buttes Formation, Dugan Pond, Sierra City Quadrangle, California. *Abs. with Prog. Geol. Soc. Am.* **6**, 139.

Best, M. G. 1963. Petrology and structural analysis of metamorphic rocks in the southwestern Sierra Nevada Foothills, California. *Univ. Calif. Publs geol. Sci.* **42**, 111–158.

Bond, G. C. & Devay, J. C. 1980. Pre-Upper Devonian quartzose sandstone in the Shoo Fly Formation, northern California—Petrology, provenance, and implications for regional tectonics. *J. Geol.* **88**, 285–308.

Boudier, F. 1978. Structure and petrology of the Lanzo peridote massif (Piedmont Alps). *Bull. geol. Soc. Am.* **89**, 1574–1591.

Burchfiel, B. C. & Davis, G. A. 1981. Triassic and Jurassic tectonic evolution of the Klamath Mountains–Sierra Nevada geologic terrane. In: *The Tectonic Development of California* (edited by Ernst, W. G.). Prentice-Hall, New Jersey, 50–70.

Clark, L. D. 1960. Foothills fault system, western Sierra Nevada, California. *Bull. geol. Soc. Am.* **71**, 483–496.

Clark, L. D. 1964. Stratigraphy and structure of part of the western Sierra Nevada belt. *Prof. Pap. U.S. geol. Surv.* **110**, 1–70.

Clark, L. D. 1976. Stratigraphy of the north half of the western Sierra Nevada metamorphic belt, California. *Prof. Pap. U.S. geol. Surv.* **923**, 1–26.

Clark, L. D. & Huber, N. K. 1975. Geologic observations and sections along selected stream traverses, north Sierra Nevada metamorphic belt, California. *Map U.S. geol. Surv.* MF-690.

Cobbold, P. R. & Quinquis, H. 1980. Development of sheath folds in shear regimes. *J. Struct. Geol.* **1**, 119–126.

Coward, M. P., Graham, R. H., James, P. R. & Wakefield, J. 1973. A structural interpretation of the northern margin of the Limpopo orogenic belt, Southern Africa. *Phil. Trans. R. Soc.* **A273**, 487–491.

D'Allura, J., Moores, E. & Robinson, L. 1977. Paleozoic rocks of the northern Sierra Nevada: their structural and paleogeographic significance. In: *Paleozoic Paleogeography of the Western United States* (edited by Stewart, J., Stevens, C. & Fritsche, A.) Society of Economic Paleontologists and Mineralogists, Pacific Section, Pacific Coast Paleogeography Symposium **1**, 394–408.

Darot, M. & Bouchez, J. L. 1976. Study of directional data distributions from principal preferred orientation axes. *J. Geol.* **84**, 239–247.

Davis, G. A. 1969. Tectonic correlations, Klamath Mountains and western Sierra Nevada, California. *Bull. geol. Soc. Am.* **80**, 1095–1108.

Davis, G. A., Monger, J. W. H. & Burchfiel, B. C. 1978. Mesozoic construction of the Cordilleran 'collage', central British Columbia to central California. In: *Mesozoic Paleogeography of the Western United States* (edited by Howell, D. & McDougall, K.) Society of

Economic Paleontologists and Mineralogists, Pacific Section, Pacific Coast Paleogeography Symposium **2**, 1–32.
Devay, C. J. & Stanley, E. 1979. Radiolaria from the Devonian Elwell Formation, northern Sierra Nevada, California (abstract). *Abs. with Prog. geol. Soc. Am.* **11**, 412.
Durrell, C. & D'Allura, J. 1977. Upper Paleozoic section in eastern Plumas and Sierra Counties, northern Sierra Nevada, California. *Bull. geol. Soc. Am.* **88**, 844–852.
Ehrenberg, S. M. 1975. Feather River ultramafic body, northern Sierra Nevada, California. *Bull. geol. Soc. Am.* **86**, 1235–1243.
Escher, A. & Watterson, J. 1974. Stretching fabrics, folds and crustal shortening. *Tectonophysics* **22**, 223–231.
Evernden, J. F. & Kistler, R. W. 1970. Chronology of emplacement of Mesozoic batholith complexes in California and western Nevada. *Prof. Pap. U.S. geol. Surv.* **623**, 1–42.
Fleuty, M. J. 1964. The description of folds. *Proc. geol. Ass.* **75**, 461–489.
Flinn, D. 1962. On folding during three-dimensional progressive deformation. *Q. Jl geol. Soc. Lond.* **118**, 385–428.
Gay, N. C. & Weiss, L. E. 1974. The relationship between principal stress directions and the geometry of kinks in foliated rocks. *Tectonophysics* **21**, 287–300.
Ghosh, S. K. 1982. The problem of shearing along axial plane foliations. *J. Struct. Geol.* **4**, 63–67.
Girty, G. H. & Wardlaw, M. S. 1984. Was the Alexander terrane a source of feldspathic sandstones in the Shoo Fly Complex, Sierra Nevada, California? *Geology* **12**, 339–342.
Hannah, J. L. & Verosub, K. L. 1980. Tectonic implications of remagnetized upper Paleozoic strata of the northern Sierra Nevada. *Geology* **8**, 520–524.
Harland, W. B. 1971. Tectonic transpression in Caledonian Spitsbergen. *Geol. Mag.* **108**, 27–42.
Hietanan, A. 1981. Geology west of the Melones Fault between the Feather and North Yuba Rivers, California. *Prof. Pap. U.S. geol. Surv.* **1226A**, 1–35.
Hudleston, P. J. 1973a. Fold morphology and some geometrical implications of theories of fold development. *Tectonophysics* **16**, 1–46.
Hudleston, P. J. 1973b. The analysis and interpretation of minor folds developed in the Moine rocks of Monar, Scotland. *Tectonophysics* **17**, 89–132.
Hudleston, P. J. & Stephansson, O. 1973. Layer shortening and fold-shape development in the buckling of single layers. *Tectonophysics* **17**, 299–321.
Kamb, W. B. 1959. Ice petrofabric observations from Blue Glacier, Washington, in relationship to theory and experiment. *J. Geol.* **64**, 1891–1909.
Karlstrom, K. E. & Houston, R. S. 1984. The Cheyenne belt: analysis of a Proterozoic suture in southern Wyoming. *Precambrian Res.* **25**, 415–446.
Kistler, R. W. 1966. Structure and metamorphism in the Mono Craters Quadrangle, Sierra Nevada, California. *Bull. U.S. geol. Surv.* **1221E**.
Matthews, P. E., Bond, R. A. B. & Van Den Berg, J. J. 1971. Analysis and structural implications of a kinematic model of similar folding. *Tectonophysics* **12**, 129–154.
McMath, V. E. 1966. Geology of the Taylorsville area, northern Sierra Nevada, California. *California Division of Mines Bull.* **190**, 173–183.
Menzies, M., Blanchard, D. & Xenophontos, C. 1980. Genesis of the Smartville arc-ophiolite, Sierra Nevada foothills, California. *Am. J. Sci.* **280A**, 329–344.
Moores, E. M. 1970. Ultramafics and orogeny, with models of the U.S. Cordillera and the Tethys. *Nature, Lond.* **228**, 837–842.
Moores, E. M. & Day, H. W. 1984. Overthrust model for the Sierra Nevada. *Geology* **12**, 416–419.
Mukhopadhyay, D. 1965. Effects of compression on concentric folds and mechanism of similar folding. *J. geol. Soc. India* **6**, 27–41.
Nicolas, A., Bouchez, J. L., Blaise, J. & Poirier, J. P. 1977. Geological aspects of deformation in continental shear zones. *Tectonophysics* **42**, 55–73.
Nicolas, A. & Boudier, F. 1975. Kinematic interpretation of folds in alpine-type peridotites. *Tectonophysics* **25**, 233–260.
Paterson, S. R. & Redfield, T. F. 1984. Finite strains and structures across the Melones fault zone near Moccasin, California (abstract). *Abs. with Progr. geol. Soc. Am.* **16**, 619.
Ramsay, J. G. 1967. *Folding and Fracturing of Rocks*. McGraw-Hill, N.Y.
Roeder, D. H. 1973. Subduction and orogeny. *J. geophys. Res.* **78**, 5005–5024.
Russell, L. 1977. Tectonic character of the Melones fault zone, western Sierra Nevada. Unpublished Ph.D. thesis, Texas Technical University, Lubbock, Texas.
Russell, S. & Nokleberg, W. 1977. Superposition and timing of deformation in the Mount Morrison roof pendant and in the central Sierra Nevada, California. *Bull. geol. Soc. Am.* **88**, 335–354.
Saleeby, J. 1977. Fracture zone tectonics, continental margin fragmentation and emplacement of the Kings–Kaweah ophiolite belt, southwest Sierra Nevada, California. In: *North American Ophiolites* (edited by Coleman, R. & Irwin, W.) *Oregon Dept. Geol. Min. Industries Bull.* **95**, 141–160.
Saleeby, J. 1978. Kings River ophiolite, southwest Sierra Nevada foothills, California. *Bull. geol. Soc. Am.* **89**, 617–636.
Saleeby, J. 1981. Ocean floor accretion and volcanoplutonic arc evolution of the Mesozoic Sierra Nevada. In: *The Geotectonic Development of California* (edited by Ernst, W. G.). Prentice-Hall, New Jersey, 132–181.
Schweickert, R. A. 1974. Probable late Paleozoic thrust fault near Sierra City, California (abstract). *Abs. with Progr. geol. Soc. Am.* **6**, 251.
Schweickert, R. A. 1976. Early Mesozoic rifting and fragmentation of the Cordilleran orogen in the western United States. *Nature, Lond.* **260**, 586–591.
Schweickert, R. A. 1981. Tectonic evolution of the Sierra Nevada range. In: *The Geotectonic Development of California* (edited by Ernst, W. G.). Prentice-Hall, New Jersey, 87–131.
Schweickert, R. A., Bogen, N. L., Girty, G. H., Hanson, R. E. & Merguerian, C. 1984. Timing and structural expression of the Nevadan orogeny, Sierra Nevada, California. *Bull. geol. Soc. Am.* **95**, 967–979.
Schweickert, R. A. & Cowan, D. S. 1975. Early Mesozoic tectonic evolution of the western Sierra Nevada, California. *Bull. geol. Soc. Am.* **86**, 1329–1339.
Schweickert, R. A. & Snyder, W. 1981. Paleozoic plate tectonics of the Sierra Nevada and adjacent regions. In: *The Geotectonic Development of California* (edited by Ernst, W. G.). Prentice-Hall, New Jersey, 182–202.
Shackleton, R. M. & Ries, A. C. 1984. The relation between regionally consistent stretching lineations and plate motions. *J. Struct. Geol.* **6**, 111–117.
Sibson, R. H., White, S. H. & Atkinson, B. K. 1981. Structure and distribution of fault rocks in the Alpine fault zone, New Zealand. In: *Thrust and Nappe Tectonics* (edited by McClay, K. R. & Price, N. J.). *Spec. Publs geol. Soc. Lond.* **9**, 197–210.
Standlee, L. A. 1978a. Middle Paleozoic ophiolite in the Melones fault zone, northern Sierra Nevada, California. *Abs. with Progr. geol. Soc. Am.* **10**, 148.
Standlee, L. A. 1978b. Geology of the northern Sierra Nevada basement rocks, Quincy-Downieville area, California. Unpublished Ph.D. thesis, Rice University, Texas.
Taliaferro, N. L. 1942. Geologic history and correlation of the Jurassic of southwestern Oregon and California. *Bull. geol. Soc. Am.* **53**, 71–112.
Thiessen, R. L. & Means, W. D. 1981. Classification of fold interference patterns: a re-examination. *J. Struct. Geol.* **2**, 311–316.
Tobisch, O. T. & Fiske, R. S. 1976. Significance of conjugate folds and crenulations in the central Sierra Nevada, California. *Bull. geol. Soc. Am.* **87**, 1411–1420.
Tobisch, O. T., Fiske, R. S., Sacks, S. & Taniguchi, D. 1977. Strain in metamorphic volcaniclastic rocks and its bearing on the evolution of orogenic belts. *Bull. geol. Soc. Am.* **88**, 23–40.
Tobisch, O. T. & Fiske, R. S. 1982. Repeated parallel deformation in part of the eastern Sierra Nevada, California and its implications for dating structural events. *J. Struct. Geol.* **4**, 177–195.
Tuminas, A. C. 1983. Geology of the Grass Valley–Colfax region, Sierra Nevada, California. Unpublished Ph.D. thesis, University of California, Davis.
Varga, R. J. 1980. Structural and tectonic evolution of the early Paleozoic Shoo Fly Formation, northern Sierra Nevada, California. Unpublished Ph.D. thesis, University of California, Davis.
Varga, R. J. 1982. Implications of Palaeozoic phosphorites in the northern Sierra Nevada. *Nature, Lond.* **9**, 217–220.
Varga, R. J. & Moores, E. M. 1981. Age, origin and significance of an unconformity that predates island-arc volcanism in the northern Sierra Nevada. *Geology* **9**, 512–518.
Weiss, L. E. 1953. Tectonic features of the Hecla Hoek to the south of St. Jonsfjorden, Vest Spitsbergen. *Geol. Mag.* **90**, 273–286.
Weiss, L. E. 1959. Geometry of superposed folding. *Bull. geol. Soc. Am.* **70**, 91–106.
Wood, D. S. 1974. Current views of the development of slaty cleavage. *A. Rev. Earth Planet. Sci.* **2**, 369–401.

APPENDIX 1

Figure		N	CI	A	E	STD	MAX	BA	BP
2									
Traverse IV	*F1A*	2	—	—	—	—	—	—	—
	F1P	2	—	—	—	—	—	—	—
	S	50	2, 4, 10, 16	0.15	7.63	2.54	18.5	1° N73° E	75 S15° E
	F2A	43	2, 4, 20, 14	0.17	7.44	2.48	14.9	56° N18° W	5 S66° W
	F2P	43	2, 4, 10, 16	0.17	7.44	2.48	16.5	2° N78° E	79 N25° W
	L	6	—	—	—	—	—	—	—
	F3A	5	—	—	—	—	—	—	—
	F3P	5	—	—	—	—	—	—	—
Lake Basin region	*F1A*	15	—	—	—	—	—	—	—
	F1P	15	—	—	—	—	—	—	—
	S	157	2, 4, 20, 40	0.05	8.51	2.84	41.9	6° N83° E	3 S7° E
	F2A	56	2, 4, 6, 8, 10	0.14	7.75	2.59	10.8	38° S4° W	8 N80° E
	F2P	56	2, 4, 10, 20	0.17	7.44	2.48	21.7	8° N83° E	37 N14° W
	L	20	2, 4, 6, 8	0.31	6.21	2.07	9.2	35° S1° E	13 N81° E
Traverse III	*S*	61	2, 4, 10, 20	0.13	7.84	2.61	20.7	3° S62° W	84 N14° E
	F2A	44	2, 4, 10, 16	0.17	7.47	2.49	16.1	83° S50° E	4 S77° W
	F2P	44	2, 4, 10, 16	0.17	7.47	2.49	16.9	2° S64° W	84 S60° E
	L	7	—	—	—	—	—	—	—
	F3A	24	—	—	—	—	—	—	—
	F3P	24	—	—	—	—	—	—	—
Traverse II	*S**	109	2, 4, 10, 20	0.08	8.31	2.77	22.7	2° S58° W	57° N32° W
	*F2A**	18	—	—	—	—	—	—	—
	*F2P**	18	—	—	—	—	—	—	—
	*L**	37	2, 4, 8	0.20	7.24	2.41	10.4	80° N10° W	3 N70° E
	F3A	9	—	—	—	—	—	—	—
	F3P	9	—	—	—	—	—	—	—
Traverse I	*S*	23	2, 4, 6, 8	0.28	6.47	2.16	9.7	27° N29° E	9 S57° E
	F2A	3	—	—	—	—	—	—	—
	F2P	3	—	—	—	—	—	—	—
	L	14	—	—	—	—	—	—	—
	F3A	14	—	—	—	—	—	—	—
	F3P	11	—	—	—	—	—	—	—
5									
	F1A	17	—	—	—	—	—	—	17° S38° W
	F1P	17	—	—	—	—	—	—	—
	S	400	2, 4, 20, 30	0.02	8.50	2.96	40.6	6° N71° E	71° N26° W
	F2A	164	2, 4, 8, 8, 16	0.05	8.53	2.84	21.4	82° N14° W	3° N74° E
	F2P	164	2, 4, 20, 30	0.05	8.53	2.84	21.4	5° N72° E	81° N46° W
	L	84	2, 4, 8, 10	0.10	8.13	2.71	11.1	73° N01° E	8 N72° E

Stereoplot statistics:
N, number of observations; CI, contours in multiples of standard deviation from an assumed random distribution; A, counting cell area (percent of plot); E, expected number of observations within A for a random distribution; STD, standard deviation; MAX, maximum STD within A; BA, best-fit axis through data; BP, pole to best-fit great-circle through data.
* Stereoplot contains data from area of Traverse II which has been rotated 40° in a clockwise manner about a vertical axis from original measured orientation. See text for explanation.